Proceedings of the DETC'99
1999 ASME Design Engineering Technical Conferences
September 12-15, 1999, Las Vegas, Nevada

DETC99/VIB-8213

DYNAMICS OF WASHING MACHINES: MECHANICAL MODEL AND SIMULATION

Falk Wagner
Lehrstuhl B für Mechanik
Technische Universität München
85747 Garching, Germany
Email: wagner@lbm.mw.tu-muenchen.de

Friedrich Pfeiffer
Lehrstuhl B für Mechanik
Technische Universität München
85747 Garching, Germany
Email: pfeiffer@lbm.mw.tu-muenchen.de

ABSTRACT

This paper deals with the dynamical behavior of washing machines. Due to large unbalance forces of the laundry during the spinning process a mechanical model has been established from d'ALAMBERT's principle that considers both the rigid body motion and the elastic vibrations. According to the complexity of the machine parts the results of a finite element mode shape analysis are used to describe the elastic behavior. The distinct bodies of the system are linked together through linear and nonlinear force elements resulting in the excitation of several machine orders. In order to verify the model, simulation results are compared with measurements.

INTRODUCTION

In recent years the requirements on washing machines with respect to maximum spinning speed and comfort have been continuously increased and, concurrently, the development expenses decreased. In order to maintain competitiveness, nowadays computer simulations become more and more popular to support this task. The aim of the research project, which is partially presented in this paper, is to develop a simulation tool, that is specifically designed for washing machines. Due to the low eigenfrequencies of some of the bodies in addition with large oscillating unbalance forces the program has to be able to consider these bodies as elastic structures.

The problem with elastic bodies compared to systems consisting of rigid bodies only is that the dynamical behavior is not represented by ordinary but partial differential equations. A detailed presentation on elastic multibody systems can be found in Bremer (1992). Johanni (1984) describes an algorithm to automatically generate the equations of motion for tree like structures with elastic beams based on d'ALAMBERT's principle using splines as shape functions for a RITZ separation. Ouatouati, Fisette, and Johnson (1997) present a program for elastic multibody systems with plates using similar approaches. However, for more complex bodies it is not possible to specify valid shape functions in such a way. Franz (1993) discusses the dynamical behavior of an electronic scale employing the eigenfrequencies and mode shapes of a finite element analysis. Sorge (1993) describes a procedure to incorporate the dynamical stiffening effects that are neglected when directly utilising finite element results. Instead of using such results he directly incorporates the mathematical description of the finite elements into its equations of motion. Wallrapp and Schwertassek (1991) propose a method which uses additional results from static finite element analyses to consider the geometrical stiffening effects.

MECHANICAL MODEL

The washing machine used to validate the mechanical model consists of a rotating drum for the laundry which is embedded in a surrounding tub. It is driven by a motor which is also mounted onto the tub. The motion of the motor is transmitted through a belt with a gear ratio of 11.25. The tub itself is suspended in the cabinet through three linear springs, a large door gasket, and two friction

dampers with additional rubber bearings. The cabinet is placed on the floor with four feet.

Since many parts of the machine are rigidly connected through screws or welding points, the whole system can be modeled using four different bodies. On the one hand, this leads to shorter computing times in the multibody simulation but on the other hand requires very complex finite element models of the elastic bodies for representing the modal parameters correctly. Figure 1 illustrates the distinct bodies of the washing machine and their attached coordinate systems. Additionally, the machine is separated

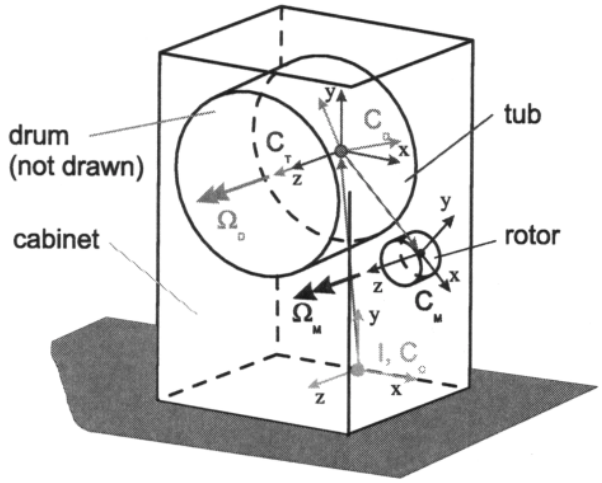

Figure 1. Mechanical model

into two subsystems which are not kinematically connected. This model has the advantage, that each subsystem is represented through an own block in the mass matrix and can be treated independently. The first subsystem consists of the tub, the drum and the rotor, the second one of the cabinet only.

The equations of motion are linearised with respect to the large rotations Ω of the drum and the rotor (see Figure 1), which leads to a non-constant mass matrix for subsystem 1 and a constant one for subsystem 2. Due to the block structure of the mass matrix only the corresponding non-constant part has to be inverted during the time integration which reduces the computational efforts.

The tub system allows all six rigid body degrees of freedom (dof), whereas the drum and the rotor have no extra dof with respect to the tub. Deviations from the given large angular velocity Ω can be considered through measured speed profiles which also include the influences from the motor controller. The cabinet is modeled without any rigid body dof. Additionally the tub, the drum, and the cabinet can be modeled elastically.

MATHEMATICAL MODEL

Equations of motion

As mentioned, the equations of motion are derived with respect to a large overall rotation of the drum and all resulting vibrations of the machine are assumed to be small. Figure 2 illustrates an arbitrary elastic body in its initial and its deformed state. In order to describe its motion several coordinate systems are associated with the body, the reference system R, a body fixed system B, and a system P to describe the behavior of arbitrary points of the body. These are for example attachment points of force elements or connections to additional bodies. Since results of a finite element analysis are used for the elastic vibrations, which are only known in a body fixed coordinate system, the equations of motion are written with respect to system B. The motion of an arbitrary point is then given by the vector chain $\boldsymbol{r}_{IR} + \boldsymbol{r}_{RB} + \boldsymbol{x}_0$ representing the rigid body movements, superimposed by elastic vibrations $\overline{\boldsymbol{r}}_{el}$. Taking the time derivatives yields the kinematical equations below

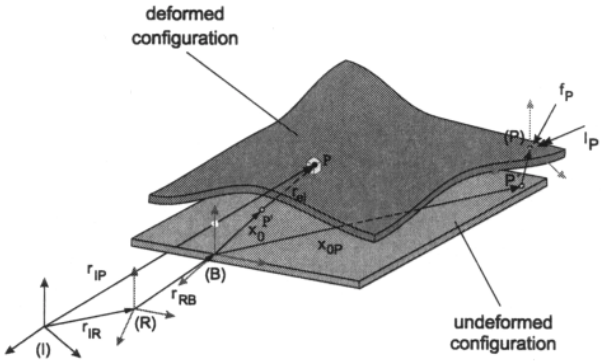

Figure 2. Coordinate systems

$$\boldsymbol{r} = \boldsymbol{r}_{IR} + \boldsymbol{r}_{RB} + \boldsymbol{x}_0 + \overline{\boldsymbol{r}}_{el}$$
$$\boldsymbol{v} = \boldsymbol{v}_a + \dot{\overline{\boldsymbol{r}}}_{el} + \tilde{\omega}(\boldsymbol{x}_0 + \overline{\boldsymbol{r}}_{el})$$
$$\boldsymbol{a} = \boldsymbol{a}_a + \ddot{\overline{\boldsymbol{r}}}_{el} + \dot{\tilde{\omega}}(\boldsymbol{x}_0 + \overline{\boldsymbol{r}}_{el}) + 2\tilde{\omega}\dot{\overline{\boldsymbol{r}}}_{el} + \tilde{\omega}\tilde{\omega}(\boldsymbol{x}_0 + \overline{\boldsymbol{r}}_{el}),$$

with $\boldsymbol{\omega}$ being the angular velocity of system B with respect to system R and $\dot{\boldsymbol{\omega}}$ being the corresponding angular acceleration. These equations are necessary to derive the

equations of motion of the elastic multibody system using d'ALAMBERT's principle according to LANGRANGE's formulation

$$\sum \int_{m_i} \delta \boldsymbol{r}^T (\boldsymbol{a} - \boldsymbol{f}) dm = 0.$$

$\boldsymbol{a}$ is the absolute acceleration as stated above, $\delta \boldsymbol{r}^T$ is a small virtual displacement of a mass element dm consistent with the kinematics of the corresponding body and $\boldsymbol{f}$ are applied forces acting on the mass element. Expanding the different terms of this equation yields the well known formulation for linearised discrete systems

$$(\boldsymbol{M}_0 + \overline{\boldsymbol{M}})(\ddot{\boldsymbol{q}}_0 + \ddot{\overline{\boldsymbol{q}}}) - (\boldsymbol{h}_0 + \overline{\boldsymbol{h}}) = \boldsymbol{0}.$$

$\boldsymbol{M}$ is the mass matrix of the system, $\boldsymbol{q}$ the vector of generalised coordinates and $\boldsymbol{h}$ includes all active forces. The index 0 indicates zeroth order, the overline first order components. Of particular interest for the derivation is the treatment of the partial differential equations describing the elastic motion of a body represented by the vector $\overline{\boldsymbol{r}}_{el}$. Therefore, the time and space dependencies are separated using a RITZ approximation

$$\overline{\boldsymbol{r}}_{el} = \boldsymbol{W} \boldsymbol{q}_{el}, \quad \boldsymbol{W} \in \mathbb{R}^{3,n}, \; \boldsymbol{q}_{el} \in \mathbb{R}^n, \; n \in \mathbb{N},$$

where $\boldsymbol{W}$ are given shape functions (here nodal components of eigenvectors) satisfying the geometrical boundary conditions and $\boldsymbol{q}_{el}$ are time dependent weighting coefficients. Using finite element models which contain elements with linear dof only the equation above leads to a correct representation of the elastic vibrations, whereas elements with angular dof or attached masses with inertia effects are not fully considered. This results from the fact that only the linear components of the eigenvector are utilised in this expression. Due to the complexity of the washing machine bodies, the models used to describe the elastic behavior consist of brick elements with three linear dof at each node, shell and beam elements with three linear and three angular dof as well as attached masses. Therefore, additional terms have to be incorporated. A later consideration of additional masses within the multibody formulation is also possible, but results in shape vectors that do not correspond with the eigenvectors of the complete body. In order to ensure convergency, more shape functions have to be used which results in longer computing times.

Introducing the RITZ separation into d'ALAMBERT's principle and considering the discrete formulation of the finite element results leads to matrices based on sums over the whole body that describe the interaction between rigid body motions and elastic deformations. These matrices can be assembled using simple summation statements

$$\int_i x_{0\alpha} W_\beta^T dm \; , \; \int_i W_\alpha^T W_\beta dm \quad \Rightarrow$$

$$\sum_i x_{0\alpha} W_\beta^T \Delta m \; , \; \sum_i W_\alpha^T W_\beta \Delta m \quad , \alpha, \beta = x, y, z,$$

that have to be carried out over all nodes of the finite element mesh (Johanni 1984, Franz 1993). $x_{0\alpha}$ are the components of an arbitrary node of the finite element mesh in its undeformed configuration (see Figure 2) and W_α are the component vectors of the employed mode shapes. Δm represent the nodal masses, resulting from an HRZ lumping (Cook, Malkus and Phlesha, 1989). These matrices will be called elementary matrices. A way for incorporating the neglected dof is illustrated in Figure 3, showing an elastic body which consists of an elastic and a rigid part connected to an element node. The vector x_0 indicates the position of

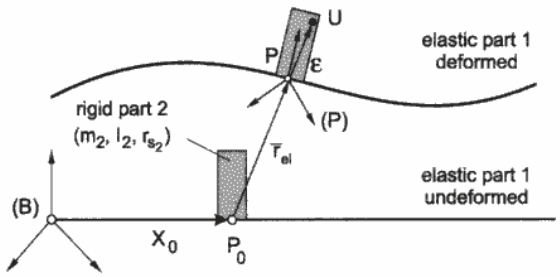

Figure 3. Elastic body with attached rigid body

the element node in its undeformed shape, $\overline{\boldsymbol{r}}_{el}$ is the elastic deformation of the node and $\boldsymbol{\varepsilon}$ the vector to an arbitrary point U of the rigid body written with respect to coordinate system P. The position of point U with respect to coordinate system B is then given by

$$(\boldsymbol{x}_0 + \boldsymbol{W}\boldsymbol{q}_{el}) + \left(\boldsymbol{E} + (\widetilde{\boldsymbol{\Phi}\boldsymbol{q}_{el}})\right) \boldsymbol{\varepsilon} \;\Leftrightarrow\; (\boldsymbol{x}_0 + \boldsymbol{\varepsilon}) + (\boldsymbol{W} - \tilde{\boldsymbol{\varepsilon}}\boldsymbol{\Phi})\, \boldsymbol{q}_{el},$$

where $\boldsymbol{\Phi}$ contains the corresponding angular nodal components of the employed mode shapes. Applying this ex-

panded expression for instance to the equations for the elementary matrix below yields

$$\int_i x_{0x} W_y^T \Delta m \Rightarrow \int_i (x_{0x} + \varepsilon_x) \left(W_y^T - ([\varepsilon_z \; 0 \; -\varepsilon_x] \boldsymbol{\Phi})^T \right) \Delta m.$$

Considering the definitions of the center of gravity and the inertia tensor as well as the discrete finite element results this equation becomes

$$\sum_i \left(\Delta m \, x_{0x} \left(W_y^T - ([r_{Sz} \; 0 \; -r_{Sx}] \boldsymbol{\Phi})^T \right) + \Delta m \, r_{Sx} - \left[-i_{xz} \; 0 \; -\frac{1}{2} (-i_{xx} + i_{yy} + i_{zz}) \right] \right).$$

With this procedure all elementary components of the matrices describing couplings between rigid body and elastic vibrations can be expanded. The additional terms include components of the vector to the center of gravity as well as the components of the inertia tensor of the attached rigid part. In the case of beam or shell elements without additional masses this equation can be simplified, since the vector to the center of gravity decays to zero.

With these adjustments a formulation has been derived that enables the usage of beam and shell elements as well as attached masses within the finite element model, and considers the particularities of these elements in the equations of motion for elastic multibody systems.

Finite element models

In the present model of the machine, the tub, the drum, and the cabinet can be modeled elastically. Figure 4 and 5 show the finite element models for the tub and the drum.

The finite element model of the tub demonstrates the utilisation of all the different element types explained above. The tub itself is modeled through 8 node shell elements, the bearing unit and the concrete counter weight through 20 node brick elements. The stator of the motor is incorporated through an attached mass that is connected to the bearing unit through 2 node beam elements with increased stiffness and reduced density. Instead of beams, so called rigid link elements can be used (MARC 1997), which results in convergency problems.

The drum model is of similar complexity compared to the tub. The drum uses 8 node shell elements, the drumstar 20 node brick elements, and the shaft 2 node beam elements, whereas the pulley is only considered through an attached mass. The influence due to an unbalance of the laundry is also taken into account.

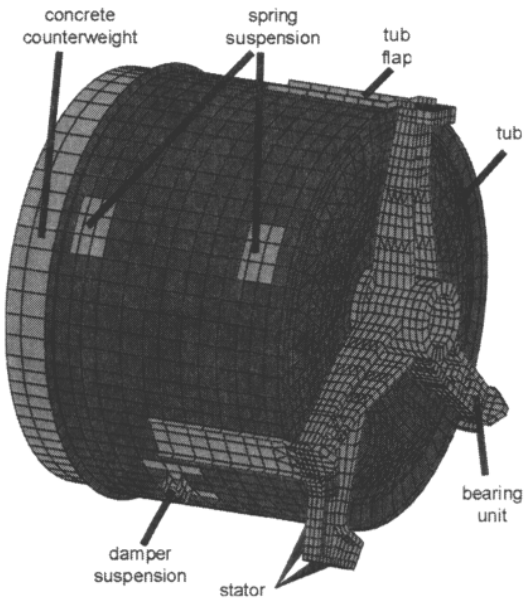

Figure 4. FE model of tub

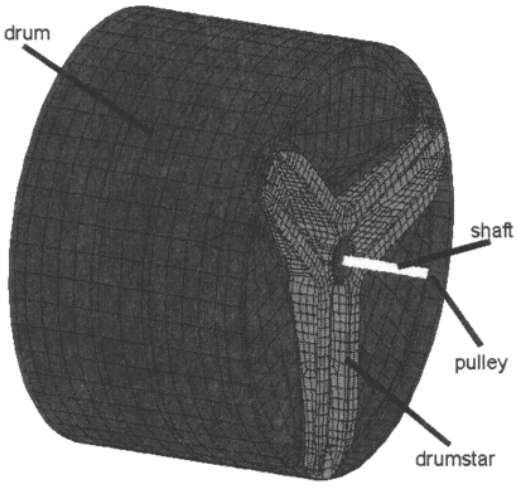

Figure 5. FE model of drum

The cabinet which is not imaged here is modeled using shell and beam elements. Due to inaccuracies during the manufacturing process the side panels of the cabinet cannot be modeled flat as featured in the technical drawing, but with a small cavity to consider the enhancement of the eigenvalues. The interaction between the cabinet and the floor is regarded by linear springs for the same reason.

Since the RITZ separation requires shape functions satisfying the geometrical boundary conditions, the finite element analysis has to be carried out with the same rigid body dof as in the later multibody simulation.

Force elements

The different bodies of the machine are connected through three different types of force elements. For the springs a linear force law is used, allowing reaction forces only in spring direction.

Friction damper

The friction damper significantly influences the dynamical behavior of the machine. Its main task is to reduce the rigid body motions of the tub in the lower speed range for avoiding contact with the cabinet. As an unwanted side effect it excites higher machine orders due to the nonlinear coherence between velocity and damping force. Especially, in higher speed ranges this leads to elastic vibrations of the tub and the cabinet. In addition, the damper consists of two rubber bearings which are considered to be linear due to the small displacements. Figure 6 shows a friction damper which is typically used in washing machines.

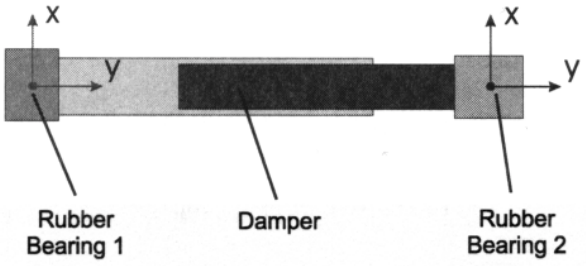

Figure 6. Friction damper with rubber bearings

One way to consider the different effects of the damper is to separate it into two independent bodies. The problem with this ad hoc solution is the mass of the tub and the drum being about one hundred times higher than the dampers mass which leads to very poor conditioned differential equations. The model presented here neglects the dynamics of the damper and uses only kinematical relations to describe it as a single massless force element.

Assuming that the rubber bearings cannot transfer any forces due to translatory motions and that the damper has no torsional stiffness with respect to its y-axis (see Figure 6), the force element can be stated using two angular degrees of freedom for each rubber bearing and one linear for the friction damper.

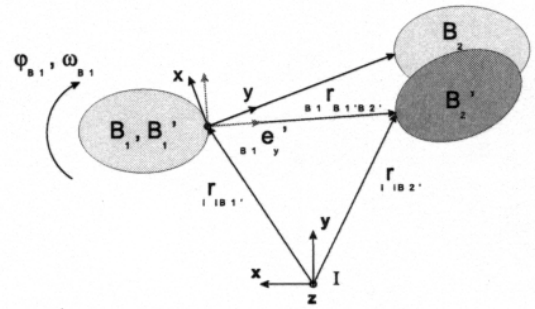

Figure 7. Kinematics of the friction damper

Figure 7 illustrates a damper attached between two bodies, whereas one body is assumed to be translatory fixed for simplicity. B_i indicates the bodies in their initial and B_i' in a deformed configuration. The transformation matrix $\boldsymbol{A}$ from coordinate system B_1' to system B_1 is given by the columnwise disposition of the unit vectors of B' written with respect to B. Since all deformations were assumed to be small the transformation matrix can be linearised as

$$\boldsymbol{A}_{BB'} = E + \widetilde{\boldsymbol{\Delta\varphi}} = [\boldsymbol{e}_{x'}, \boldsymbol{e}_{y'}, \boldsymbol{e}_{z'}].$$

The unit vector in y'-direction of rubber bearing 1 with respect to the coordinate system of the undeformed configuration is given by

$${}_{B_1}\boldsymbol{e}_{y_{B_1'}} = \frac{{}_{B_1}\boldsymbol{r}_{B_1'B_2'}}{|{}_{B_1}\boldsymbol{r}_{B_1'B_2'}|} = \begin{pmatrix} -\gamma \\ 1 \\ \alpha \end{pmatrix} \Rightarrow \boldsymbol{\Delta\varphi} = \begin{pmatrix} \alpha \\ 0 \\ \gamma \end{pmatrix}.$$

Thus, with the unit vector described above the angular displacements of bearing 1 can be derived, where α and γ are rotations with respect to the x- and z-axis of the bearing.

For the required velocities of the force element a similar approach becomes feasible, but the equations are now written with respect to the deformed configuration. The relative linear velocity between attachment points B_1' and B_2' is given by the equation below where $\boldsymbol{r}$ is an abbreviation of ${}_{B_1'}\boldsymbol{r}_{B_1'B_2'}$ and $\boldsymbol{\omega}$ is the relative angular velocity of the two points

$${}_{B_1'}\boldsymbol{\Delta v}_{B_1'B_2'} = \dot{\boldsymbol{r}} + \tilde{\boldsymbol{\omega}}\boldsymbol{r} = \begin{pmatrix} v_x \\ v_y \\ v_z \end{pmatrix}.$$

Evaluating the two terms of this equation separately and taking the angular velocity of body 1 into account yields the desired velocities of bearing 1 and the friction damper

$$\begin{pmatrix} 0 & -\omega_z & 0 \\ \omega_z & 0 & -\omega_x \\ 0 & \omega_x & 0 \end{pmatrix} \begin{pmatrix} 0 \\ r \\ 0 \end{pmatrix} = \begin{pmatrix} -\omega_z r \\ 0 \\ \omega_x r \end{pmatrix} = \begin{pmatrix} v_x \\ 0 \\ v_y \end{pmatrix}$$

$$\Rightarrow \boldsymbol{\Delta\omega} = \frac{1}{r} \begin{pmatrix} v_z \\ 0 \\ -v_x \end{pmatrix} - \boldsymbol{\omega}_{B_1} \ , \ \dot{\boldsymbol{r}} = \begin{pmatrix} 0 \\ v_y \\ 0 \end{pmatrix}.$$

The kinematical values for bearing 2 are obtained using the same procedure.

The force law of the rubber bearings consists of two linear rotary spring-damper statements

$$\boldsymbol{M}_{1,2} = \boldsymbol{C}_{1,2}\boldsymbol{\Delta\varphi}_{1,2} + \boldsymbol{D}_{1,2}\boldsymbol{\Delta\omega}_{1,2},$$

whereas a nonlinear law is invoked for the friction damper. In order to avoid a system with unilateral contacts COULOMB's friction law is approximated through an arc tangent function, yielding the force law below.

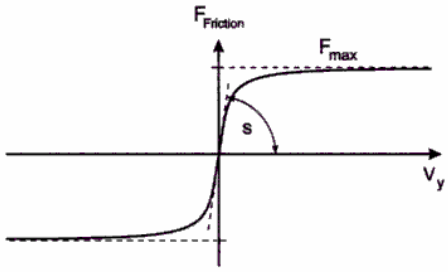

$$F_{Friction} = \frac{2F_{max}}{\pi} \arctan(sv_y)$$

Figure 8. Friction law

The forces acting on the bodies due to the bending moments within the bearings can be derived from the static equilibrium of the complete damper.

Door gasket

The door gasket is modeled as a six dimensional spring-damper element. Due to its complex geometry a finite element analysis has to be carried out to determine the coefficients of the stiffness matrix. Mooney-Rivlin material is used to describe the rubber.

The analysis is done applying all possible displacements in separate runs onto the model and calculating the necessary reaction forces and moments. The influences of superimposing several displacements concurrently are not investigated. Since the calculated effects due to geometrical and material nonlinearities within the range of interest are small, the characteristic curves are finally linearised. The achieved stiffness matrix is of non-diagonal shape.

Since only a static analysis is performed, the damping coefficients of the force element have to be determined through an adaptation between simulations and measurements.

RESULTS

In order to verify the mechanical model a very detailed experimental investigation of the washing machine was carried out (Meys 1998). The examination was done using a magnet with a mass of 0.6 kg to simulate an unbalance due to the laundry. Since the position of the laundry within the drum is of importance as well, three different locations were investigated (see Figure 9). For a comparison of the results

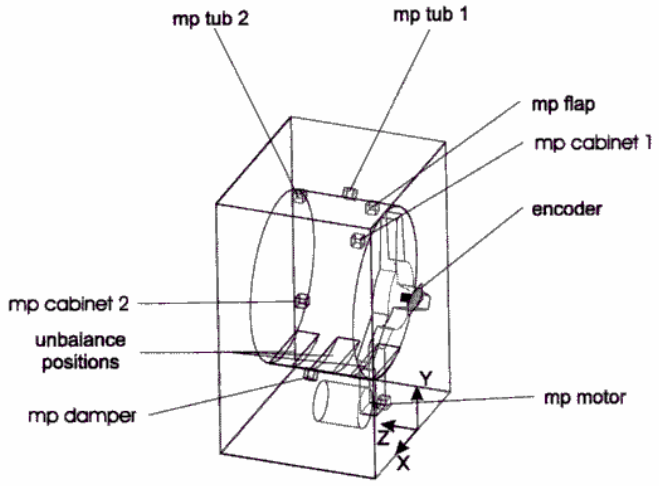

Figure 9. Experimental setup

presented below, a position of the unbalance in the front of

the drum was chosen. All studies were performed, taking the large angular speed of the drum as system input and measuring the linear accelerations during a stationary run-up on seven different points on the machine, five located on the tub and two on the cabinet (abbreviated with mp in Figure 9). The speed range between a minimal adjustable value and the maximum spinning speed was subdivided into three regions. The lower one is of interest for the rigid body resonances of the tub and any influences due to elastic vibrations are neglectible. The intermediate region is of subsidiary interest, since only a few elastic modes of the cabinet with very small magnitudes are excited due to the nonlinear behavior of the friction damper. The third range is of particular interest for the elastic vibrations. On the one hand large, even visible oscillations of the cabinets side panel are excited and on the other hand the additional unbalance of the motor excites vibrations in an audible frequency band due to the gear ratio of 11.25.

Since the reference value for all measurements is the angular velocity of the drum, cascade plots respectively order plots were established for evaluating the results.

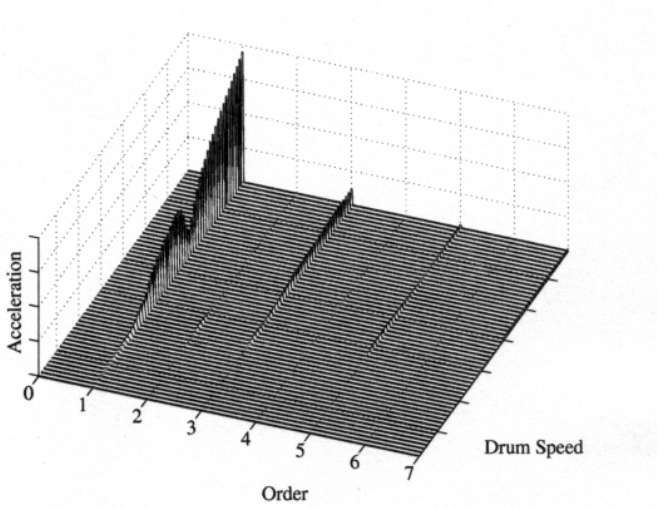

Figure 10. Order plot Acceleration x-Direction: Comparison of measurement (left) and simulation (right) on mp tub 2

Rigid Body Model

A comparison of the linear accelerations on measurement point tub 2 in the lower speed range is shown in Figure 10, to demonstrate the quality of the rigid body model and the modeling of the force elements. The calculation of the measured fast fourier transforms (FFT) was done applying a HANNING-window to avoid leakage effects, which bisects the real magnitudes. Afterwards an energy correction was performed to preserve the total energy of the measured time signal and the transformed one according to PARSEVAL's theorem. The still existing differences in the resulting magnitudes were finally removed by multiplication with a constant factor. Due to this second correction the total energy of the measured system is not preserved and the different spectra within the measured order plot appear to be wider than the simulated ones.

It is obvious, that the simulation matches quite well with the measurement, both qualitatively and quantitatively. The excitation of higher orders results from the nonlinearities of the friction damper. Additionally, the shape of the first order is strongly influenced by the door gasket, which legitimates the modeling efforts.

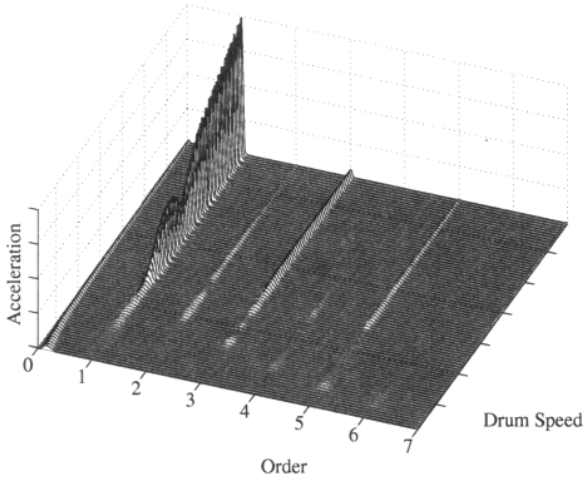

Elastic Deformations of the Drum

The first eigenfrequency of the drum is too high to be excited by the unbalance forces. Figure 11 shows the static displacement of the front of the drum over the complete speed range. The parabolic shape of the curve results from the fact that the unbalance force increases with Ω^2, where Ω is the speed of the drum. Due to the modeling technique of the drum, the static displacement is superimposed by a small oscillation.

The calculation of the drum deformation is a very important design criterion leading to large stresses within the material and even to the failure of the structure. One advantage of the introduced modeling technique is that the RITZ approximation can be reversed and applied as boundary conditions to the finite element model to calculate the stresses. Figure 12 exhibits the deformation of the finite

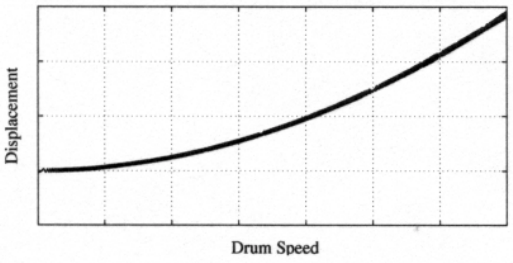

Figure 11. Elastic displacement of the drum

element model of the drum, which have been recalculated from the applied mode shapes and the simulation results.

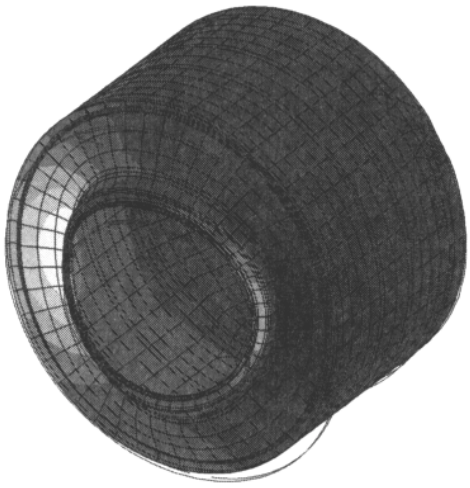

Figure 12. FE model of the drum displacements

Elastic Vibrations of the Cabinet

Finally, the elastic vibrations of the cabinet are presented. The design parameters of the force elements of the machine are chosen in a way that deformations of the tub barely excite elastic vibrations of the cabinet. Thus, the tub can be modeled as a rigid body and the motor unbalance can be neglected.

The interaction between the feet of the cabinet and the floor is considered in the finite element model by springs. In order to receive comparable results with the measurements it is necessary that all four feet are equally loaded. Figure 13 compares the measured and the simulated acceleration in x-direction at point cabinet 2 which is in the center of the side panel.

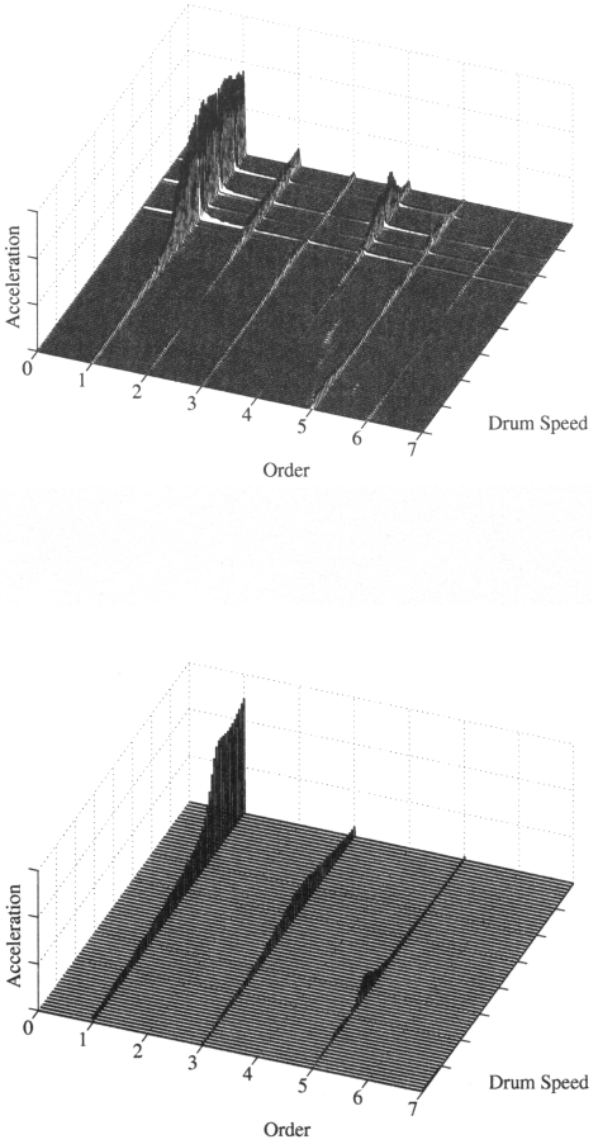

Figure 13. Order plot acceleration x-direction: comparison of measurement (top) and simulation (bottom) on mp cabinet 2

Especially the first eigenfrequency is important, as it is leading to large, even visible displacements. The vibrations are basically excited by the friction damper and the door gasket, since the resulting spring forces act mainly in the plane of the side panels. Thus, displacements perpendicular to the plane result from effects of second order and can be neglected for the present configuration (9). The missing even orders in the simulation result from the fact that the

only nonlinearity in the current model comes from the friction damper which has an odd FOURIER series expansion.

One effect of the side panel that can only be seen in the speed plot is shown in Figure 14. Obviously, the acceleration is not symmetric to the x-axis of the plot which results from the bended shape of the side panel. Due to this the stiffnesses in positive and negative direction are not the same. This effect can be regarded in the simulation by applying characteristic curves rather than the eigenfrequencies of the modal analysis to assemble the stiffness matrix of that body.

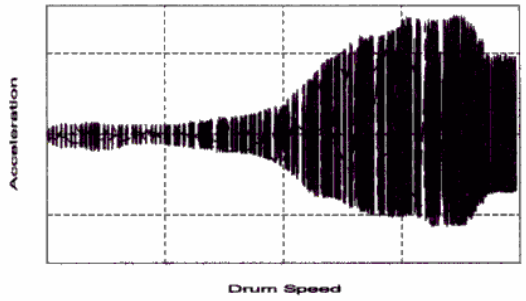

Figure 14. Speed plot measured acceleration x-direction

CONCLUSION

The presented model of a washing machine as an elastic multibody system enables the analysis of the vibrational behavior, excited by the unbalance of the laundry and the motor. The simulation results determine the friction damper as the main source for the excitation of higher machine orders. The absence of some even machine orders point out that additional nonlinearities have to be incorporated into the present model. One improvement can be found in a more detailed representation of the connection between the tub and the concrete counterweight (see Figure 4), which is currently modeled as a rigid link.

Additionally, the utilisation of finite element results as shape functions for a RITZ separation provide the possibility of recalculating the stresses within the material.

REFERENCES

H. BREMER, F. PFEIFFER *Elastische Mehrkörpersysteme, Teubner Studienbücher, Stuttgart 1992*

R. COOK, D. MALKUS, M. PHLESHA *Concepts and Applications of Finite Element Analysis, third edition, John Wiley & Sons Inc, 1989*

E. FRANZ *Dynamik von elektromechanischen Präzisionswaagen, Lehrstuhl B für Mechanik, TU München, Dissertation 1993*

R. JOHANNI *Automatisches Aufstellen der Bewegungsgleichungen von baumstrukturierten Mehrkörpersystemen mit elastischen Körpern, Lehrstuhl B für Mechanik, TU München, Diplomarbeit 1984*

LMS International *MIRAS, Roadrunner User Guide, Revision 3.84*

MARC Analysis Research Corporation *User Manual, Volume A - D, 1997*

M. MEYS *Experimentelle Schwingungsanalyse einer Waschmaschine, Lehrstuhl B für Mechanik, TU München, Semesterarbeit 1998*

A. EL OUATOUATI, P. FISETTE, D.A. JOHNSON*A Fully Symbolic Model of Multibody Systems Containing Flexible Plates, University of Louvain-la-Neuve, Department of Mechanical Engineering, 1997*

K. SORGE *Mehrkörpersysteme mit starr-elastischen Subsystemen, Lehrstuhl B für Mechanik, TU München, Dissertation 1992*

O. WALLRAPP, R. SCHWERTASSEK *Representation of Geometric Stiffening in Multibody System Simulation, International Journal for Numerical Methods in Engineering, vol. 32, 1991*